

# Controlling amine receptor group density on aluminum oxide surfaces by mixed silane self assembly

Ilsoon Lee, Richard P. Wool\*

*Department of Chemical Engineering, University of Delaware, Newark, DE 19716, USA*

Received 25 April 2000; received in revised form 25 July 2000; accepted 31 August 2000

## Abstract

To estimate adhesion at polymer–solid interfaces, model substrates with varying  $-\text{NH}_2$  density on  $\text{Al}_2\text{O}_3$  were prepared by a self-assembly of mixed amine terminated silanes (AS) and methyl terminated silanes (MS). The density of  $-\text{NH}_2$  groups on  $\text{Al}_2\text{O}_3$  was varied by changing the mol.% of AS and MS in solution. The model surfaces were characterized by means of X-ray photoelectron spectroscopy (XPS), contact angle measurements, atomic force microscopy (AFM), and mechanical tests with polymers. The analysis of the competitive coadsorption kinetic model showed that MS adsorbed two times faster than AS on aluminum surfaces. The surface energetics of  $\text{Al}_2\text{O}_3$  was controlled by the mixed silane treatments from hydrophobic and low energetic to hydrophilic and high energetic surfaces. © 2000 Elsevier Science B.V. All rights reserved.

**Keywords:** Polymer–solid interfaces;  $-\text{NH}_2$  groups;  $\text{Al}_2\text{O}_3$ ; Silanes

## 1. Introduction

The self-assembly of organic monolayers (SAMs) on substrates have been intensively studied since first described by Zisman et al. [1]. The focus of interest has been long chain alkylthiols on gold and long chain alkyl-trichlorosilanes on oxidized surfaces such as silicone, glass, and metal. Due to their important industrial applications in catalysts, sensors, and adhesives, an understanding of the properties and behavior of these materials on the molecular scale has become of great importance. Critical issues of these materials have been how to control and stabilize them as well as the determination of the molecular scale structures. The

SAM-substrates have become a tool for tethering molecules like antibodies, proteins, etc. to solid substrates [2,3]. Our studies, which focussed on adhesion, controlled the density of receptor groups using a mixed self assembly for a polymer–solid adhesion study [4]. The incompatibility of hydrophobicity or hydrophilicity between a polymer and a solid surface can be overcome through many industrial techniques such as laser, plasma, and ozone treatments [5]. These treatments improve the strength of the polymer–solid interface. However, the uncertainty of the molecular scale structures prepared by these techniques makes it difficult to understand the receptor density effect on polymer adhesion on a molecular level. Therefore, to obtain more defined surfaces, we prepared self-assembled monolayers of mixed amine-terminated silanes (AS) and methyl-terminated silanes (MS) for the polymer adhesion study. Small chain alkyl silanes were chosen for self-assembling for their wide acceptance in polymer–solid adhesion.

\* Corresponding author. Tel.: +1-302-831-3312; fax: +1-302-831-8525.

E-mail addresses: lee@che.udel.edu (I. Lee), wool@ccm.udel.edu (R.P. Wool).

The structural difference between the two silanes is that AS has a primary polar  $\text{NH}_2$  group, whereas MS has a less polar  $\text{CH}_3$  group at the terminal carbon chain. Thus, MS was used to decrease the substrate active receptor groups ( $-\text{NH}_2$ ) via competitive adsorption reaction from the mixed solutions on  $\text{Al}_2\text{O}_3$ . As shown in Fig. 1, the methoxy groups ( $-\text{OCH}_3$ ) of the silanes were hydrolyzed to form silanol-containing species  $[-\text{Si}(\text{OH})_3]$ . The silanol-containing species were highly reactive intermediates, which were responsible for bond formation with the substrate functional groups ( $\text{Al}-\text{OH}$ ). The general mechanism for silane bond formation has been well explained [6,7]. During the hydrolysis and condensation reactions followed by the silane deposition, the first layer was strongly anchored to  $\text{Al}_2\text{O}_3$  by the surface reaction of the silanol containing species with the surface functional groups ( $\text{Al}-\text{OH}$ ). However, the other layers were physically and weakly deposited on the first layer at solid–liquid interfaces before the rinsing procedure. The weakly deposited layers were not appropriate for the polymer adhesion study, since they might complicate the failure mode of the interface. The careful rinsing procedure was performed to develop so-called ‘self-assembled monolayers’ (SAMs).

## 2. Experimental

### 2.1. Preparation

The model-substrates with varying density of  $-\text{NH}_2$  (0–100 mol.%) on  $\text{Al}_2\text{O}_3$  were prepared using a self-assembly of mixed amine-terminated silanes [AS;  $\gamma$ -aminopropyltrimethoxy silane;  $\text{H}_2\text{NCH}_2\text{CH}_2\text{CH}_2\text{Si}(\text{OMe})_3$ ] and methyl-terminated silanes [MS;  $n$ -propyltrimethoxy silane;  $\text{CH}_3\text{CH}_2\text{CH}_2\text{Si}(\text{OMe})_3$ ]. The details of silane self-assembly are well known [7]. The Al

foil, purchased from Shim Stock Inc., was first pre-treated overnight at  $300^\circ\text{C}$  in an oven to ensure the formation of a stable layer of native oxide. The thickness of the Al foil was  $25\text{ }\mu\text{m}$  and the roughness average (RA) was determined to be approximately  $0.5\text{ }\mu\text{m}$  using a scanning white light interferometer (SWLI). The total combined concentrations of AS and MS in the mixed silane water solutions were  $50\text{ mM}$  (ca.  $0.8\text{ wt.}\%$ ). The pH of the solutions was maintained at 4.5 for all solution concentrations using acetic acid. To apply silane coatings, the samples were dipped in solution for 5 min. The silane-treated substrates were rinsed with copious amounts of distilled water to prepare monolayer-like silane coatings. After rinsing, the monolayer-like silane coatings were dried at room temperature for 1 h and then cured in an oven under  $\text{N}_2$  purging at  $115^\circ\text{C}$  for 30 min. The surface composition was determined by X-ray photoelectron spectroscopy (XPS). In addition, an atomic force microscope (AFM) and a dynamic contact angle analyzer were used to further characterize the model substrates. The thickness of the silane coatings was uniform regardless of surface concentrations. However, it was not clear whether the model-surfaces were monolayers, so they will be called ‘monolayer-like silane coatings’ in this paper.

### 2.2. XPS

The surface composition of the model-substrates was analyzed by a Leybold–Heraeus XPS. This system has a monochromatic  $\text{Mg K}\alpha$  X-ray source ( $h\nu = 1253.6\text{ eV}$ ). The pressure in the sample chamber was maintained at approximately  $10^{-9}$  torr. Based on the Si peak intensities, the coverage or the thickness of the silane coatings on  $\text{Al}_2\text{O}_3$  was determined not to be a function of the receptor ( $-\text{NH}_2$ ) density. In addition,

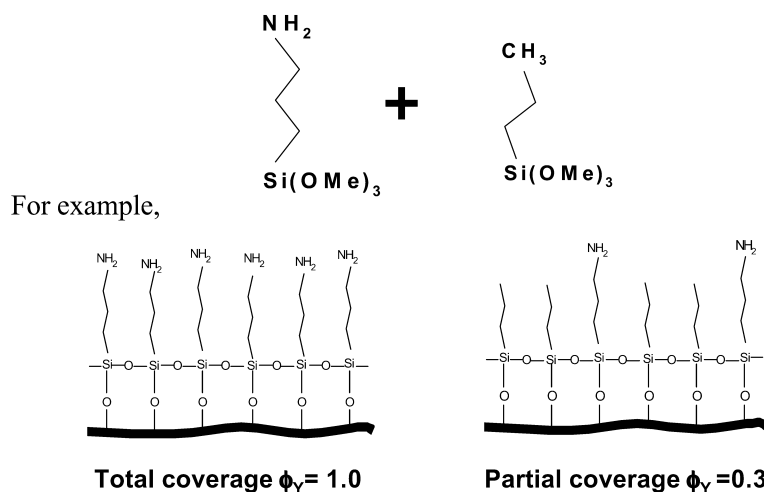


Fig. 1. Schematic representation of the preparation of mixed silane coatings on  $\text{Al}_2\text{O}_3$ .

based on the relative peak intensity of N1s and Si2p peaks, the surface composition was determined.

### 2.3. Contact angle

The surface wetting properties of the monolayer-like silane coatings on  $\text{Al}_2\text{O}_3$  were investigated with a CAHN dynamic contact angle analyzer using a Wilhelmy plate technique. Thicker aluminum foil (Shim Stock Inc., thickness of 250  $\mu\text{m}$ ) was used for monolayer-like silane coatings on  $\text{Al}_2\text{O}_3$ . The thick Al foils were cut into small pieces ( $24 \times 50 \times 0.25$  mm). The Al pieces were coated with silanes using the preparation methods described in the above section of preparation. The plate-moving speed was 22  $\mu\text{m/s}$ .

### 2.4. AFM

The silane coverage and two-dimensional distribution of AS and MS in the mixed monolayer-like silane coatings on  $\text{Al}_2\text{O}_3$  were explored with an atomic force microscope (AFM) in Tapping Mode<sup>TM</sup>. A silicon probe with dimension of  $125 \times 3 \times 1$   $\mu\text{m}$  and a tip radius of 5–10 nm was oscillated at its mode-1 resonance frequency and setpoint voltage between 50 and 55% of the free vibrational amplitude in air. The difference between the setpoint and the free amplitude was directly related to the amount of force applied to the surface during the imaging. To verify surface structures observed with AFM, untreated  $\text{Al}_2\text{O}_3$  surfaces was also imaged.

### 2.5. Adhesion

The effect of the surface treatment on adhesion to carboxylated polybutadiene (cPBD) was tested. The cPBD contained approximately 3 mol.%  $-\text{COOH}$  sticker groups randomly distributed along the polybutadiene (PBD) backbone chain with  $M_n = 98000$  and  $M_w = 180000$ . The fracture energy,  $G_{IC}$ , of the cPBD-AIS interfaces was evaluated using a T-peel test. A layer of cPBD was uniformly cast from a 2-wt.% solution in toluene onto the coated substrate. The thickness of the cPBD was estimated to be 16  $\mu\text{m}$ , based on volume of solution cast, surface area covered, and weight gain. After the toluene was evaporated under vacuum for 15 min, another coated substrate was used to form an AIS-cPBD-AIS sandwich structure. After being pressed together to ensure good contact, the AIS-cPBD-AIS structure was annealed under 4 kPa pressure at room temperature for different times. The jointed substrates were cut into specimens with dimensions of 60 mm in length and 10 mm in width. The peel tests were conducted on a Mini-44 Instron tensile machine at a crosshead speed of 30 mm/min. The fracture energy,  $G_{IC}$ , was obtained from the average of

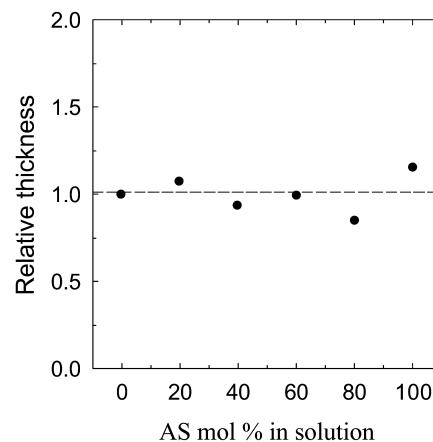


Fig. 2. Relative thickness of the mixed monolayer-like silane coatings.

three tests per material and is given by:

$$G_{IC} = \frac{2P}{b} \quad (1)$$

where  $P$  is the peel load and  $b$  is the width of the test sample.

## 3. Results and discussion

### 3.1. XPS analysis

The XPS spectrum gave an average composition of the entire silane layers, more or less weighted to the surface, since Al peaks were also observed. It was assumed that most of the available Al-OH groups on  $\text{Al}_2\text{O}_3$  were taken by either the AS or MS silanes. To confirm the uniform thickness or uniform coverage of the monolayer-like silane coatings, the relative Si peak intensities at various amine receptor group densities,  $\phi_Y$ , were compared using Eq. (2):

Relative thickness or coverage

$$= \frac{I(\text{Si2p})}{I(\text{Si2p})|_{(\text{MS})}} \quad (2)$$

where  $I$  is the peak intensity of the atomic component on the coated-substrates. Fig. 2 shows that the relative Si peak intensities were approximately constant as  $\phi_Y$  was varied. The sampling depth of XPS is 40–100 Å, and the length of an AS molecule is approximately 8 Å. The monolayer-like silane coatings, showing weak Si peaks and strong Al peaks, were prepared and used in this work. However, the silane multilayers showing strong N and Si peaks and weak Al peaks, as shown in Fig. 3, which were prepared without the rinsing procedure, were used in the determination of the surface composition. The random distribution of AS was as-

sumed in the silane multilayers. The overlayer and the buried overlayer models, which will be discussed later, were not assumed to represent the AS distribution. It was known that the degradation of the top surfaces at a molecular level had normally been observed during XPS scanning in an ultra high vacuum chamber [8]. A very weak N1s peak but relatively strong Si peak of the monolayer-like silane coating by the pure AS coating was detected, even though the atomic sensitivity of N1s is greater than that of Si2p peaks. We suspect that the X-ray degraded the  $-\text{NH}_2$  layer exposed to it, but it did not degrade much of the anchoring atoms (Si) due to the greater depth of the Si. That is why we used the silane multilayers to determine the composition, which made it possible to detect every distinct peak, as shown in Fig. 3. This is correct as long as the random distribution of AS in the multilayers is assumed. The surface composition was determined using Eq. (3) and the detailed XPS component scans as shown in Fig. 4:

$$\phi_Y(\text{NH}_2) = \phi(\text{AS}) = \frac{\frac{I(\text{N1s})}{I(\text{Si2p})} - \frac{I(\text{N1s})}{I(\text{Si2p})}|_{(\text{MS})}}{\frac{I(\text{N1s})}{I(\text{Si2p})}|_{(\text{AS})} - \frac{I(\text{N1s})}{I(\text{Si2p})}|_{(\text{MS})}}. \quad (3)$$

Due to the different atomic sensitivities and the positions from the coating surface between N and Si atoms, the composition was normalized as shown in Eq. (3). For example  $\phi_Y$  of the pure AS treated substrates is 1, and that of a pure MS treated substrate is 0. Hence, the composition of the mixed layers is between 0 and 1. It must be noted that carbon (C) was the main atomic component of impurities normally found on high energetic surfaces, and one AS molecule contained one Si atom and one N atom, while one MS molecule had one Si atom but no N atom.

### 3.2. Contact angle analysis

Fig. 5 shows the water advancing contact angle,  $\theta_a$

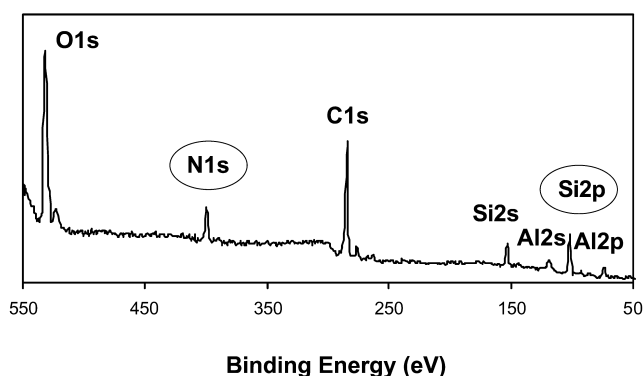


Fig. 3. XPS spectrum of AS multilayers on  $\text{Al}_2\text{O}_3$ .

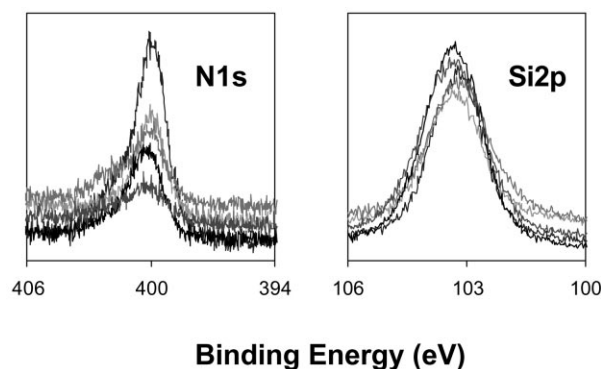


Fig. 4. XPS peaks of N1s (left) and Si2P (right) of the mixed silane multilayers of AS and MS.

( $\text{H}_2\text{O}$ ), of the surfaces vs. AS mol.% on surface, respectively. The surface composition was determined using XPS analysis. As shown in Fig. 5, the  $\theta_a(\text{H}_2\text{O})$  of the surface of the model substrates with the pure AS ( $\phi_Y = 1$ , total  $-\text{NH}_2$ ) was measured to be  $83.5^\circ (\pm 1.5^\circ)$  and with pure MS ( $\phi_Y = 0$ , total  $-\text{CH}_3$ ) was  $96.8^\circ (\pm 3^\circ)$ . The contact angle for the untreated  $\text{Al}_2\text{O}_3$  (total  $-\text{OH}$ ) was approximately  $43^\circ (\pm 2^\circ)$ . The mixed monolayer-like silane coatings  $0 < \phi_Y < 1$  showed large variations ( $6\text{--}11^\circ$ ) but gave  $\theta_a$  values approximately along the linear interpolation line between the pure AS and pure MS coated-substrates. Large variation of mixed monolayer-like silane coatings was also shown in other mixed self-assembled systems [9]. From the literature, the  $\theta_a(\text{H}_2\text{O})$  of monolayer-like silane coatings were reported as  $88.4^\circ (\pm 4^\circ)$  for the AS-treated surface [10]. The  $\theta_a(\text{H}_2\text{O})$  of the monolayer-like silane coatings varied with the length and packing of carbon backbone chains, as well as the terminal functional groups [11]. The  $\theta_a(\text{H}_2\text{O})$  was reported as  $102^\circ (\pm 2^\circ)$  for *n*-butyltrichlorosilane treated surface which has one more carbon chain (C4) relative to MS (C3),  $62^\circ\text{--}76^\circ$  for *tert* butyltrichlorosilane (C4) treated sur-

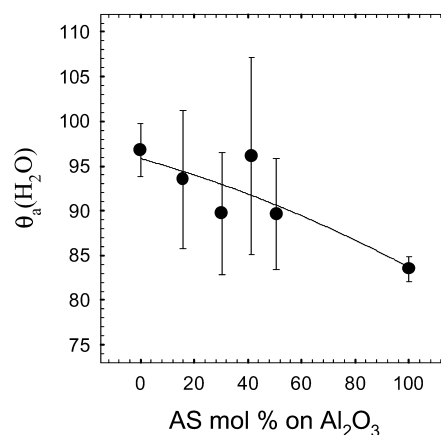


Fig. 5. Advancing water contact angles vs. AS mol.% on  $\text{Al}_2\text{O}_3$  surfaces.

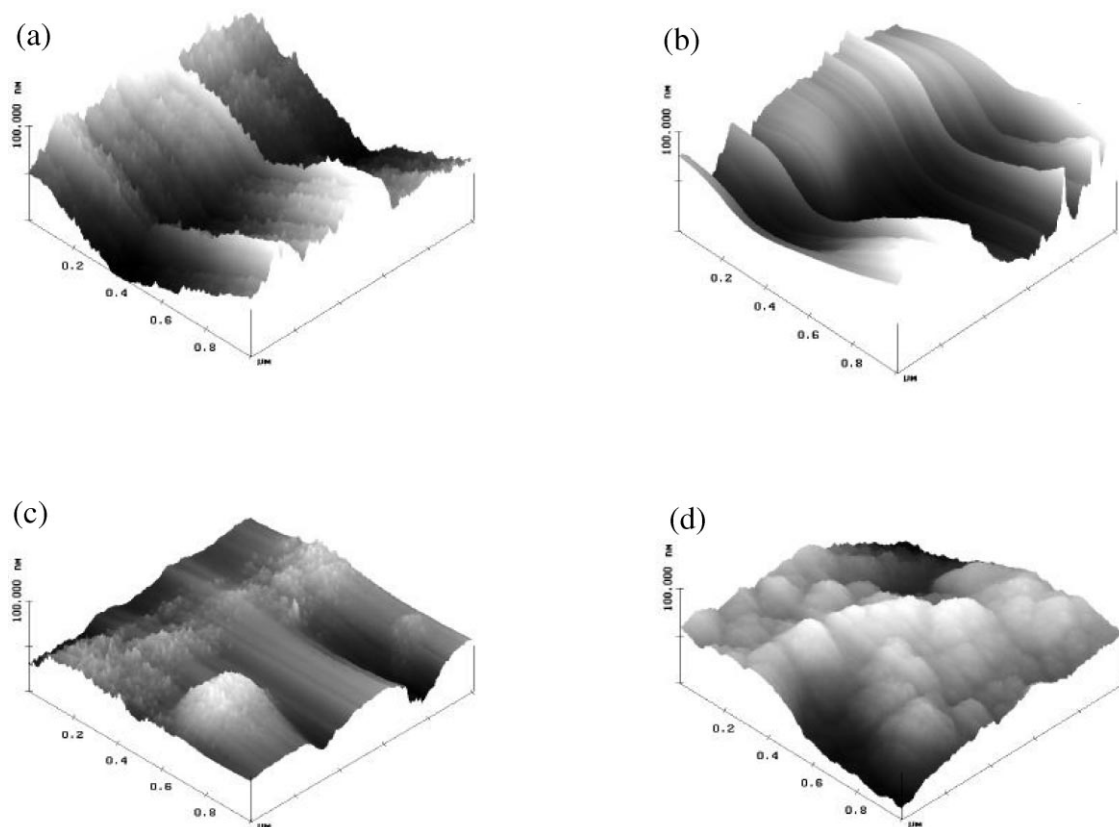


Fig. 6. AFM images of the mixed monolayer-like silane coatings on  $\text{Al}_2\text{O}_3$  surfaces. (a) Untreated  $\text{Al}_2\text{O}_3$  surfaces. (b) AS mol.% in solution = 100%. (c) AS mol.% in solution = 50% (on  $\text{Al}_2\text{O}_3$  = 30%). (d) AS mol.% in solution = 0%.

faces, and  $112^\circ (\pm 2^\circ)$  for octadecyltrichlorosilane (C18) treated surfaces.

### 3.3. AFM images analysis

Atomic force microscope (AFM) in Tapping Mode<sup>TM</sup> was used to see the silane coverage and two-dimensional distribution of AS and MS in the mixed monolayer-like silane coatings on  $\text{Al}_2\text{O}_3$ . As shown in Fig. 6, the AFM images of  $\phi_Y = 1$ ,  $\phi_Y = 0$ , and the pure  $\text{Al}_2\text{O}_3$  were clearly different from each other. This was expected because the images were made from the contact force differences between the silicon tip of AFM and the model-substrates. The AFM images of intermediate densities, between  $\phi_Y = 1$  and  $\phi_Y = 0$ , appeared to be different from those of  $\phi_Y = 1$ ,  $\phi_Y = 0$ , and the pure  $\text{Al}_2\text{O}_3$ , however, they were not clear enough to relate the images to the intermediate densities.

### 3.4. Silane layers

It was believed that the distribution of AS and MS on  $\text{Al}_2\text{O}_3$  was random. Evidence supporting this claim is as follows: the surface reaction is so fast that it can be considered random; the  $\text{Al}_2\text{O}_3$  can be completely

covered by silanes within a couple of minutes. Secondly, the surface anchoring groups of AS and MS are the same and the molecular structures of AS and MS are similar to each other except for their terminal groups. In addition, contact angle measurements further confirmed that the surface is not an overlayer or buried overlayer, because the contact angle almost varied linearly between  $\phi_Y = 1$  and  $\phi_Y = 0$ . Finally, AFM images showed that the mixed monolayer-like silane coatings did not look like one of  $\phi_Y = 1$  and  $\phi_Y = 0$ .

### 3.5. Competitive coadsorption kinetic model

Fig. 7 shows the experimental results of the solution mole fraction vs. the surface mole fraction determined by XPS analysis, where the total combined concentrations remained constant. The results were fitted using a competitive adsorption model, which is discussed below. The formation of mixed silane layers with AS and MS is dominated by kinetic effects associated with hydroxyl groups on the aluminum surface [7]. This resulted in the irreversible formation of silicon–oxygen bonds with strengths of approximately 128 kcal/mol [12]. This factor was first addressed when studying a mixed monolayer formation [9], and is equally applicable to

our system where the adsorption reaction of the silanes to the Al surfaces is quite fast. The adsorption rate of each adsorbate can be expressed by:

$$r_1^{\text{surf}} = \frac{dc_1^{\text{surf}}}{dt} = k'_1 c_1^{\text{solu}} \quad (4)$$

$$r_2^{\text{surf}} = \frac{dc_2^{\text{surf}}}{dt} = k'_2 c_2^{\text{solu}} \quad (5)$$

where  $r$ , surf, solu, and  $k$  represent adsorption rate, surface, solution, and reaction constant, respectively. The overall rate of silane layer formation is the sum of the incorporation rates of the individual adsorbates:

$$r_{\text{total}}^{\text{surf}} = \frac{dc_1^{\text{surf}} + dc_2^{\text{surf}}}{dt} = k'_1 c_1^{\text{solu}} + k'_2 c_2^{\text{solu}} \quad (6)$$

Thus:

$$\phi_2^{\text{surf}} = \frac{r_2^{\text{surf}}}{r_{\text{total}}^{\text{surf}}} = \frac{k'_2 c_2^{\text{solu}}}{k'_1 c_1^{\text{solu}} + k'_2 c_2^{\text{solu}}} \quad (7)$$

$$\phi_2^{\text{surf}} = \frac{1}{\left\{ \left( \frac{k'_1}{k'_2} \right) \left( \frac{c_1}{c_2} \right) + 1 \right\}^{\text{solu}}} \quad (8)$$

In the experiment, the concentrations,  $c_1$  and  $c_2$ , remained constant and can be converted to solution fractions,  $\phi(\text{MS})$  and  $\phi(\text{AS})$ . In addition, the adsorption reaction rates do not necessarily have a first order dependence on the solution concentration, thus, a parameter,  $n$ , can be included in Eq. (8). The competitive adsorption of AS and MS was analyzed using Eq. (9). The data were fitted to determine the model parameters  $A$  and  $n$  of this system, as shown in Fig. 7.

$$\phi^{\text{surf}}(\text{NH}_2) = \phi(\text{AS})^{\text{surf}} = \frac{1}{\left\{ A \left( \frac{\phi(\text{MS})}{\phi(\text{AS})} \right)^n + 1 \right\}^{\text{solu}}} \quad (9)$$

Here,  $A$  is the ratio of apparent surface reaction constant,  $k'_{\text{MS}}/k'_{\text{AS}}$ . The first parameter  $A$  was determined to have a value of 2 which roughly means that MS adsorbed to  $\text{Al}_2\text{O}_3$  twice as fast as AS. The second parameter  $n$  was determined to be 0.6. This means that the competitive adsorption reaction is negatively cooperative for AS; adsorbed AS molecules on  $\text{Al}_2\text{O}_3$  prevent free AS molecules in solution from adsorbing onto the next available sites. Mixed self-assembly is crucial in designing surfaces for biodetectors and in studying a cell adhesion on biological substrates. In this work, model substrates formed by a self-assembly of AS

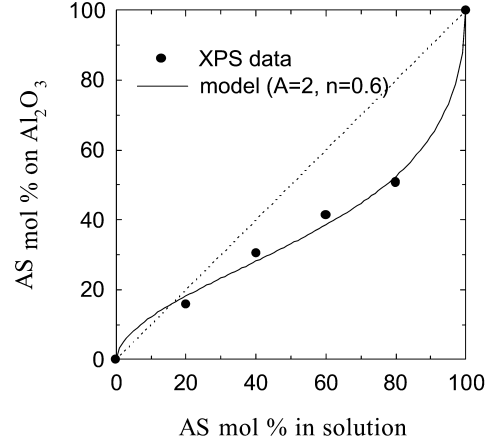


Fig. 7. AS mol.% in solution vs. AS mol.% on  $\text{Al}_2\text{O}_3$  surfaces.

and MS on  $\text{Al}_2\text{O}_3$  were used to understand the fundamentals of substrate receptor group effects on polymer adhesion.

### 3.6. Adhesion test

The fracture energy,  $G_{\text{IC}}$ , of the weak interface, the pure PBD–AIS interfaces, were determined to be approximately  $10 \text{ J/m}^2$  at all annealing times and was not a function of the substrate receptor group density. The pure PBD surfaces of low surface energy interacted with the model substrate by the weak interaction, van der Waals forces. When a few percent of sticker groups (approx. 3 mol.%) was introduced onto the pure PBD,  $G_{\text{IC}}$  showed remarkable changes with the substrate receptor group density, contrary to the case of pure PBD–AIS interfaces, as shown in Fig. 8. At short time (10 min),  $G_{\text{IC}}$  increased as the density of substrate receptor group increased, as was expected. On the other hand, at long time (1000 min)  $G_{\text{IC}}$  (1000 min) increased with increasing  $\phi_Y$  up to the critical receptor concentration,

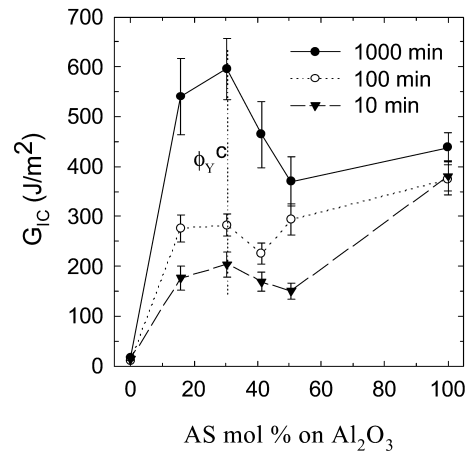


Fig. 8. Fracture energy of the cPBD–AIS interfaces,  $G_{\text{IC}}$ , as a function of receptor mol.% on  $\text{Al}_2\text{O}_3$  surfaces. The concentration of sticker group ( $-\text{COOH}$ ) was approximately 3 mol.%. The data point at AS mol.% = 0 based on the pure dispersive forces of PBD.

30 mol.%, and then it decreased with further increases in  $\phi_Y$ . The maximum  $G_{IC}$  of 600 J/m<sup>2</sup> is almost the same value with the bulk cohesive  $G_{IC}$  of PBD [13]. It can be explained that the fracture energy of the polymer–solid interface is subject to the weaker of the adhesive and cohesive strengths. When the concentration of the receptor group and the annealing time is small, increasing the receptor group concentration increases the adhesive strength. However, at high concentration, the dense attachment of the near-surface layer to the solid substrate decreased the cohesive strength. The details of this polymer adhesion study were published in another paper [4,14].

#### 4. Conclusion

Monolayer-like silane coatings were prepared on aluminum oxide surfaces with terminal amine endgroups and terminal methyl endgroups. The density of amine receptor groups on Al<sub>2</sub>O<sub>3</sub> was varied from 0 to 100 mol.% by preparing mixed self-assembled monolayers by coadsorption of amine terminated and methyl terminated silanes. The prepared mixed monolayer-like silane coatings on Al<sub>2</sub>O<sub>3</sub> surfaces were characterized by means of XPS, AFM, contact angle, and mechanical tests. These characterizations enabled the understanding of coadsorption kinetics, surface images, surface energetics, and one of their potential applications as a function of amine receptor density. The composition of the monolayer-like silane coatings on Al<sub>2</sub>O<sub>3</sub> was different from the composition of the silanization solu-

tion. The data fitting of coadsorption model indicated that the amine terminated silanes preferentially adsorbed twice as fast on Al<sub>2</sub>O<sub>3</sub> than methyl terminated silanes.

#### Acknowledgements

This work was supported by Hercules, Inc., Wilmington, Delaware and NSF-DMR-9596-267.

#### References

- [1] W.G. Bigelow, D.L. Pickett, W.A. Zisman, *J. Colloid Sci.* 513 (1946) 1.
- [2] K.L. Prime, G.M. Whitesides, *Science* 1164 (1991) 11.
- [3] A. Liebmann, L. Lander, M.D. Foster, W.J. Brittain, E.A. Vogler, S. Satija, C.F. Majkrzak, *Langmuir* 2256 (1996) 12.
- [4] I. Lee, R.P. Wool, *Macromolecules* 2680 (2000) 33.
- [5] K.L. Mittal, *Polymer Surface Modification: Relevance to Adhesion*, Utrecht, The Netherlands, 1996.
- [6] B. Arkles, *Chemtech* 766 (1977) 7.
- [7] E. Plueddemann, *Silane Coupling Agents*, Plenum, New York, 1982.
- [8] T.J. Lenk, V.M. Hallmark, J.F. Rabolt, L. Haussling, H. Ringsdorf, *Macromolecules* 1230 (1993) 26.
- [9] J.P. Folkers, P.E. Laibinis, G.M. Whitesides, *Langmuir* 1330 (1992) 8.
- [10] P.H. Harding, J.C. Berg, *J. Appl. Polym. Sci.* 1025 (1988) 67.
- [11] D.A. Offord, J.H. Griffin, *Langmuir* 3015 (1993) 9.
- [12] R. Walsh, *Acc. Chem. Res.* 246 (1981) 14.
- [13] C.M. Roland, G.G.A. Bohm, *Macromolecules* 1310 (1985) 18.
- [14] L.Z. Gong, A.D. Friend, R.P. Wool, *Macromolecules* 3706 (1998) 31.